

Modeling and Analysis of Biological Cells in DRAM Implementation

Jeffrey Fan[†], Guofen Yu[§], Jichang Tan[‡], Sheldon X.-D. Tan[◦]

[†]Department of ECE, Florida International University, Miami, Florida 33174, USA

[§]Department of Physics, University of Findlay, Findlay, Ohio 45840, USA

[‡]Department of CS and IE, St. John's University, Taipei 25135, Taiwan

[◦]Department of EE, University of California, Riverside, California 92521, USA

ABSTRACT

In this paper, we propose a novel technique in modeling and analysis of biological cells to implement DRAM storage elements in the post-CMOS era. The motivation is based on the known characteristics of biological cells. By applying an electric pulse with a fixed duration, we may calculate the voltage across the cytoplasmic membrane, also called a cell membrane or plasma membrane, and the nuclear membrane within biological cells. The induced voltage across the membranes may function like a capacitor does in a DRAM storage element. The electron charge accumulated on a membrane is also leaky, similar to the traditional DRAM. The electron charge and discharge time constants for cytoplasmic and nuclear membranes can be fine-tuned through careful selection of different sizes and types of biological cells. Experimental results by simulation show that about 75 percents (75%) of the applied voltage is distributed across the cytoplasmic membrane. Hence, cytoplasmic membrane is more suitable in the application of DRAM implementation. This means that when applying $0.9V - 1V$ of voltage across a biological cell, roughly $0.7V - 0.75V$ of the voltage is induced across the cytoplasmic membrane. The electron charge and discharge time can be achieved within 100 ns for certain size and type of biological cells. The required DRAM refresh frequency is therefore approximately 10 MHz for such biological cells.

1. INTRODUCTION

Dynamic Random Access Memory (DRAM) is the most common kind of random access memory (RAM) for personal computers and workstations. DRAM stores each bit in a storage cell consisting of a capacitor and a transistor. Since real capacitors leak charge, the information eventually fades away unless the capacitor charge is refreshed periodically. Because of this refresh requirement, it is called a dynamic memory in contrast to Static Random Access Memory (SRAM) and other static memory. Its advantage over SRAM is in its structural simplicity: only one transistor and one capacitor are required per bit, compared to six transistors in SRAM. This allows DRAM to reach very high density at a relatively low cost.

In response to the growing gap between memory access time and processor speed, DRAM manufacturers have developed several DRAM architectures in the past ten to fifteen years. Those available in the industry include Fast Page Mode [2], Extended Data Out [3], Synchronous [4], Enhanced

Synchronous [5], and Synchronous Link [6]. The study like [1] has provided a simulation-based performance evaluation of a representative group, evaluating each of these architectures in terms of its effect on total execution time.

According to the report from International Technology Roadmap for Semiconductors (ITRS) [7], the scaling of Complementary Metal Oxide Semiconductor (CMOS) technology will continue to evolve and dominate the semiconductor industry for at least another ten years. This may lead to over 14 billion transistors integrated onto a single chip with a clock frequency of over 50GHz in the 18-nanometer technology. However, what will happen in the post-CMOS era? The search for alternative technologies is certainly in demand. The focus of this paper is not the study based on the existing DRAM architectures. Instead, it emphasizes on the search of a DRAM storage cell structure that is different from and unrestricted by the MOSFET design in the traditional DRAM technology.

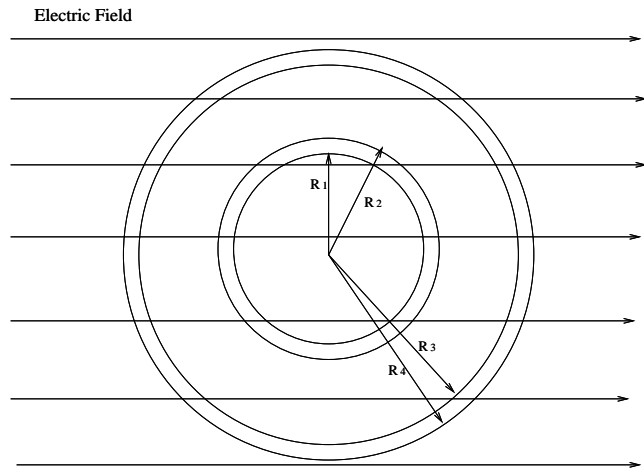


Figure 1: Multi-shell single biological cell model

In searching for the new devices, one potential technology is the use of biological cells. The membrane of a biological cell creates a large barrier to the transport of ions and charged molecules both inside and outside of cell. Such barrier may be compromised to improve the transport of ions and charged molecules by applying external physical stimulus. One typical stimulus is the application of electrical field,

i.e., voltage. Under such electrical field, there exists a voltage across the transmembrane domain, thus charge is accumulated on the transmembrane similar to the way a capacitor would respond. A pulsed electrical field is sufficient to cause the transmembrane voltage reaching $1V - 2V$. In addition, some pores on the cytoplasmic membrane may be formed under the electric field to further increase the transport of ions and charged molecules. Such phenomenon is called *electroporation* [8]. The typical usage of electroporation includes (1) the introduction of DNA, enzymes, antibodies, and other biochemical reagents for intracellular assay, (2) the introduction of virus and other particles, (3) the insertion of membrane molecules into the cell membrane, and (4) the killing of cells under nontoxic conditions. Thanks to the extensive applications, there has been intensive study of electroporation in the field of medical application (e.g., [9, 10]).

Similar to the effects of traditional DRAM, the induced voltages caused by external electric field within the biological cell are leaky. The rate of discharge of electrons depends upon the time constants of the biological cell. The amount of induced voltages across transmembrane also depend upon the type and shape of biological cell. In this paper, we show that by careful selection of the shape and size of the biological cell, the “memory” of a cell may be kept long enough so that it is comparable to traditional DRAM device made of MOSFET in terms of operation and refreshing.

The rest of this paper is organized as follows: Section 2 presents the modeling of multi-shell single biological cell and the basis of distribution of voltage in transmembrane domain. Section 3 presents the experimental results and Section 4 concludes this paper.

2. MODELING OF MULTI-SHELL SINGLE CELL

The diagram of multi-shell single biological cell is shown in Fig. 1 [11]. R_1 and R_2 are the inner and outer radii of nuclear membrane, respectively. R_3 and R_4 denote the inner and outer radii of cytoplasmic membrane, respectively. The amplitude of the applied electromagnetic wave is denoted by E_0 . The model of the biological cell is divided into five regions:

- Region I*, $0 \leq r \leq R_1$, nuclear region
 - Region II*, $R_1 \leq r \leq R_2$, nuclear membrane
 - Region III*, $R_2 \leq r \leq R_3$, cytoplasm region
 - Region IV*, $R_3 \leq r \leq R_4$, cytoplasmic membrane
 - Region V*, $r \geq R_4$, extracellular environment
- (1)

Suppose that the cell is under an electromagnetic wave with angular frequency ω . As the permeability of most biological materials is very close to that of the air, the magnetic fields can be neglected. Furthermore, the diameter of a cell (typically, $10\mu\text{m}$) is small, thus the external field, \vec{E}_{ext} , around the cell is assumed to be homogenous and uniformly applies to the cell. Thus,

$$\vec{E}_{ext} = E_0 e^{-j\omega t} \vec{z} \quad (2)$$

It is obvious to see that we have an axial-symmetric system,

i.e. in a spherical coordinate systems, r , φ , θ , and $\partial/\partial\varphi = 0$. The scalar potential, V_0 , of the applied field can be written as:

$$V_0 = -E_0 r \cos\theta = -E_0 r P_1(\cos\theta) \quad (3)$$

where $P_1(\cos\theta)$ is the first order Legendre function.

Hence, the potentials in five regions within the biological cell described in equation (1) can be written as: (A_n , $B1_n$, $B2_n$, $C1_n$, $C2_n$, $D1_n$, $D2_n$, and F_n are constants) as follows.

$$\begin{aligned} V_I &= \sum_{n=0}^{\infty} A_n r^n P_n(\cos\theta), 0 \leq r \leq R_1 \\ V_{II} &= \sum_{n=0}^{\infty} [B1_n r^{-(n+1)} + B2_n r^n] P_n(\cos\theta), R_1 \leq r \leq R_2 \\ V_{III} &= \sum_{n=0}^{\infty} [C1_n r^{-(n+1)} + C2_n r^n] P_n(\cos\theta), R_2 \leq r \leq R_3 \\ V_{IV} &= \sum_{n=0}^{\infty} [D1_n r^{-(n+1)} + D2_n r^n] P_n(\cos\theta), R_3 \leq r \leq R_4 \\ V_V &= \sum_{n=0}^{\infty} [F_n r^{-(n+1)} P_n(\cos\theta) - E_0 r P_1(\cos\theta)], r \geq R_4 \end{aligned} \quad (4)$$

Let $Z_I = \sigma_I + j\omega\varepsilon_I$, $Z_{II} = \sigma_{II} + j\omega\varepsilon_{II}$, $Z_{III} = \sigma_{III} + j\omega\varepsilon_{III}$, $Z_{IV} = \sigma_{IV} + j\omega\varepsilon_{IV}$, and $Z_V = \sigma_V + j\omega\varepsilon_V$, where σ and ε indicate the conductivity and permittivity in each region of the cell respectively. Also assume that the surface charges can be neglected. The following equations for potentials and normal current density at boundary surfaces are valid:

$$\begin{aligned} V_I &= V_{II}, \quad Z_I (\partial V_I / \partial r) = Z_{II} (\partial V_{II} / \partial r); r = R_1 \\ V_{II} &= V_{III}, \quad Z_{II} (\partial V_{II} / \partial r) = Z_{III} (\partial V_{III} / \partial r); r = R_2 \\ V_{III} &= V_{IV}, \quad Z_{III} (\partial V_{III} / \partial r) = Z_{IV} (\partial V_{IV} / \partial r); r = R_3 \\ V_{IV} &= V_V, \quad Z_{IV} (\partial V_{IV} / \partial r) = Z_V (\partial V_V / \partial r); r = R_4 \end{aligned} \quad (5)$$

Applying the orthogonality of Legendre function, it can be shown that the constants A_n , $B1_n$, $B2_n$, $C1_n$, $C2_n$, $D1_n$, $D2_n$, and F_n in the equation (4) are zeroed out when $n \neq 1$. When $n = 1$, the constants can be re-written as follows:

$$\begin{aligned} B1_1 &= \frac{3Z_V E_0}{2Z_{IV} R_4^{-3} d_1 - Z_{IV} d_2 - 2Z_V R_4^{-3} g_1} \\ A_1 &= \frac{3Z_{II}}{(Z_{II} - Z_I) R_I^3} B1_1 \\ B2_1 &= \frac{2Z_{II} + Z_I}{(Z_{II} - Z_I) R_I^3} B1_1 \\ C1_1 &= c1 B1_1 \\ C2_1 &= c2 B1_1 \\ D1_1 &= d1 B1_1 \\ D2_1 &= d2 B1_1 \\ F1_i &= g_1 B1_1 + R_4^3 E_0 \end{aligned} \quad (6)$$

where

$$\begin{aligned}
c1 &= \frac{Z_{III} + 2Z_{II}}{3Z_{III}} + \frac{(2Z_{II} + Z_I)(Z_{III} - Z_{II})R_3^3}{3Z_{III}(Z_{II} - Z_I)R_1^3} \\
c2 &= \frac{2Z_{III} - 2Z_{II}}{3Z_{III}R_2^3} + \frac{(2Z_{II} + Z_I)(2Z_{III} + Z_{II})}{3Z_{III}(Z_{II} - Z_I)R_1^3} \\
d_1 &= \frac{2Z_{III} + Z_{IV}}{3Z_{IV}}c1 + \frac{Z_{IV} - Z_{III}}{3Z_{IV}}R_3^3c2 \\
d_2 &= \frac{2(Z_{IV} - Z_{III})}{3Z_{IV}R_3^3}c1 + \frac{2Z_{IV} + Z_{III}}{Z_{IV}}c2 \\
g_1 &= d_1 + R_4^3d_2
\end{aligned} \tag{7}$$

Hence, given the applied voltage on the biological cell, the induced voltage across each regions can be obtained in the equation (6) and (7), respectively.

3. EXPERIMENTAL RESULTS

All the experimental results are implemented and simulated in Matlab. In order to investigate the response of a single cell subjective to an electric pulse, numerical simulations are carried out for typical cellular dimensions with cellular dielectric properties. The constants used in the simulation are derived from measurements by various research papers cited below.

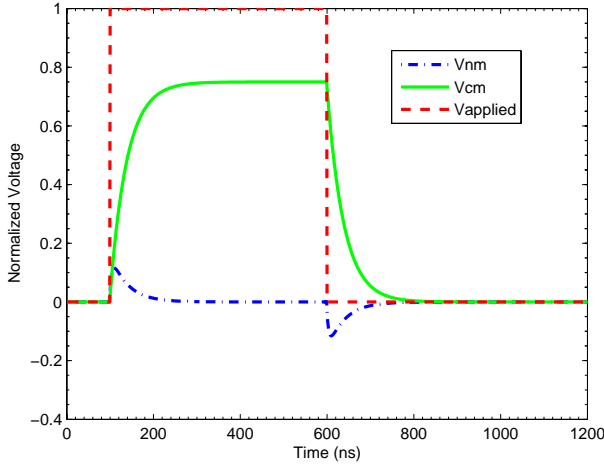


Figure 2: Response of small circular biological cell

In our calculation, the relative permittivity in the region of nucleus, cytoplasm, and extracellular media is assumed to be 81 (see [12]). This value is different in membranes whose permittivity is assumed to be 5 (see also [12]). The conductivity in nucleus, cytoplasm, and extracellular media is assumed to be 0.3 S/m [13]. However, the conductivity in the membranes is assigned with the value of $3e^{-7} \text{ S/m}$ [14]. The calculation is based on three different sizes of circular biological cells: (1) small cell, $R_1 = 0.5\mu\text{m}$, $R_3 = 2.5\mu\text{m}$, (2) medium cell, $R_1 = 1.5\mu\text{m}$, $R_3 = 3.5\mu\text{m}$, and (3) large cell, $R_1 = 2.5\mu\text{m}$, $R_3 = 5.0\mu\text{m}$. The definitions of R_1 and R_3 are the radii of the single biological cell as shown in Fig. 1.

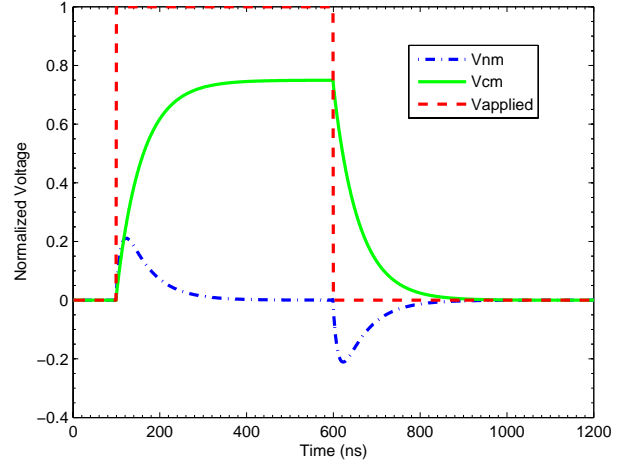


Figure 3: Response of medium circular biological cell

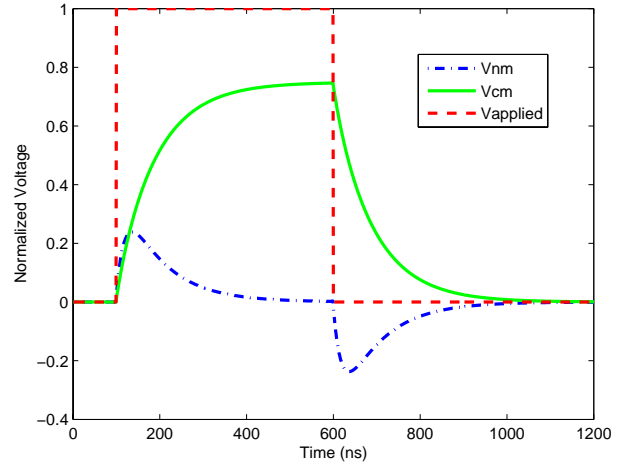


Figure 4: Response of large circular biological cell

Furthermore, the thickness of cytoplasmic membrane is assumed to be 10 nm , while the thickness of nuclear membrane is usually double in measurement, i.e. 20 nm . Figures 2, 3, and 4 show the experimental results for each simulation with various sizes of single biology cell. For each size of biological cell, the voltage is applied with electric rectangular pulse for the duration of 500ns (denoted as $V_{applied}$ in all three figures). Fig 4 is the response of the large cell. The normalized voltages across cytoplasmic membrane (denoted as V_{cm}) are shown in the figures. The normalized voltage means the percentage of membrane voltage verse the voltage applied onto the single cell. For example, the value of V_{cm} is roughly 0.75 with respect to the applied voltage in Fig. 2. This means that if the total applied external voltage is 1V , the voltage across cytoplasmic membrane is roughly 0.75V .

Similarly, the normalized voltages across nuclear membrane (denoted as V_{nm}) are shown in all three figures. It is

obvious that the voltage across cytoplasmic membrane (V_{cm}) is about 75% to 80% of the applied voltage for all three sizes of biology cells. However, the voltage across nuclear membrane (V_{nm}) is relatively small with respect to applied voltage, roughly less than 10%. This implies that the cytoplasmic membrane is a better choice acting as a capacitor than nuclear membrane in consideration of DRAM application. Furthermore, for cytoplasmic membrane, the time constant is about 40ns as shown in Fig. 2, 70ns in Fig. 3 and 100ns in Fig. 4. This indicates that time constants of the charge and discharge of electrons can be adjusted by employing different size of biological cells. In application to DRAM storage cells, the smaller time constant indicates the more frequency requirement of DRAM refresh. Clearly, the larger size of the single biological cell as shown in Fig. 4 is a better choice in application to biological DRAM in comparison to two other figures. Given the time constant of 100ns in Fig. 4, the required refresh frequency is about 10 MHz. We may choose even larger size of biological cell as DRAM storage, such as $10\mu\text{m}$ in radius. In such case, the time constant is roughly about 200ns . The cell is able to "memorize" the information longer than smaller cell. Therefore, the required refresh frequency is much less (about 5 MHz). However, the duration of the pulse of external applied electric field will need to be longer in order to fully charge the biological cell. This may be a trade-off to be considered about by the designers.

Another observation is that the electron charge and discharge time across nuclear membrane is much faster than the one in cytoplasmic membrane. There is also much less voltage induced across the nuclear membrane for a relatively short period of time (observed in terms of the charging and discharging time across the cytoplasmic membrane). This implies that we may prefer to use cytoplasmic membrane as a capacitor in the implementation of biological DRAM.

4. CONCLUSION AND FUTURE WORK

In this paper, we proposed a novel technique to implement DRAM storage elements by modeling and analyzing circular biological cells. The selection of biological cells with various shapes and sizes are explored. We investigated the characteristics of the biological cells, such as the induced voltages across nuclear and cytoplasmic membranes plus the electron charge and discharge time in these membranes under external excitations. Simulation results show that the cytoplasmic membrane is a better choice in DRAM implementation in terms of voltage induced by external electric field and the requirement of DRAM refresh. Future research shall include using of non-circular biological cells with different sizes and shapes in application to DRAM and other elements in electronic circuit design.

5. REFERENCES

- [1] V. Cuppu, B. Jacob, B. Davis, T. Mudge, "A performance comparison of contemporary DRAM architectures", IEEE International Symposium on Computer Architecture, pp. 1-12, May 1999
- [2] Samsung. FPM DRAM 4M x 16 Part No. KM416V4100C. Samsung Semiconductor, [http://www.usa.samsungsemi.com/products/prodspec/dramcomp/KM416V40\(1\)00C.PDF](http://www.usa.samsungsemi.com/products/prodspec/dramcomp/KM416V40(1)00C.PDF), 1998.
- [3] IBM. EDO DRAM 4M x 16 Part No. IBM0165165PT3C. <http://www.chips.ibm.com/products/memory/88H2011/88H2011.pdf>, 1998.
- [4] IBM. SDRAM 1M x 16 x 4 Bank Part No. IBM0364164. <http://www.chips.ibm.com/products/memory/19L3265/19L3265.pdf>, 1998.
- [5] ESDRAM. Enhanced SDRAM 1M x 16. Enhanced Memory Systems, http://www.edram.com/products/datasheets/16M_Esdram0298a.pdf, 1998.
- [6] SLDRAm. 4M x 18 SLDRAm Advance Datasheet. SLDRAm, Inc., <http://www.sldram.com/Documents/corp400b.pdf>, 1998.
- [7] Website: International technology roadmap for semiconductors, <http://www.itrs.net/>
- [8] J.C. Weaver, "Electroporation in cells and tissues: A biological phenomenon due to electromagnetic fields", Radio Science, Vol 30, No 1, pp. 205-221, 1995
- [9] S.B. Dev, D.P. Rabusay, G. Widera, G.A. Hofmann, "Medical applications of electroporation", IEEE Transactions on Plasma Science, vol 28, no 1, pp 206-223, 2000
- [10] J.M. Wells, L.H. Li, A. Sen, G.P. Jahres, S.W. Hui, "Electroporation-enhanced gene delivery in mammary tumors", Gene Therapy, Vol 7, No 7, pp. 541-547, 2000
- [11] G. Yu, Y. Gao, S. Liu, W. Wang, J. Wu, "Can Millimeter Waves Generate Electroporation?", International Journal of Infrared and Millimeter Waves, Col 23, No 8, pp. 1261-1269, 2002
- [12] I. Ermolina, Y. Polevaya, Y. Feldman, "Study of Normal and Malignant White Blood Cell by Time Domain Dielectric Spectroscopy", IEEE Transactions on DEI, Vol 8, No 2, pp. 253-261, 2001
- [13] C.M. Harris, D.B. Kell, "The radio-frequency dielectric properties of yeast cells measured with a rapid, automated frequency-domain dielectric spectrometer", Bioelectrochem Bioenergy, Vol 11, pp 15-28, 1983
- [14] P.R.C. Gascoyne, R. Pethig, J.P.H. Burt, F.F. Becker, "Membrane changes accompanying the induced differentiation of Friend murine erythroleukemia cell studied by dielectrophoresis", Biochim Biophys Acta, Vol 1146, pp. 119-126, 1993